J|A|C|S
ARTICLES
Published on Web 10/12/2004

Effect of Weak Interactions on the H···H Distance in Stretched Dihydrogen Complexes

Dmitry G. Gusev*
Contribution from the Department of Chemistry, Wilfrid Laurier University, Waterloo, Ontario N2L 3C5 Canada

Received June 9, 2004; E-mail: dgoussev@wlu.ca

Abstract: Computational and experimental results presented in this paper demonstrate that the H−H distance in stretched dihydrogen complexes can be hypersensitive to a variety of weak intra- and intermolecular interactions, including those with bulky ligands and solvent molecules, hydrogen-bonding interactions, or ion-pairing. Particularly, the complex $IrH(H\cdots H)Cl_2(P^iPr_3)_2$ which contains a stretched dihydrogen ligand in the crystalline form, as shown by neutron diffraction, is a trihydride in solution. The difference is due to the intermolecular Ir−Cl···H−Ir hydrogen bonding in the solid.

Introduction

Dihydrogen coordination to transition metals was discovered about 20 years ago.[1] Since then, many dihydrogen complexes have been reported as isolable species or reaction intermediates in the oxidative addition/reductive elimination of dihydrogen at transition-metal centers.[2] According to the conventional theoretical description, η^2-H_2 bonding involves combined forward-donation $\sigma(H_2) \rightarrow d_\sigma(M)$ and back-donation $d_\pi(M) \rightarrow \sigma^*(H_2)$.[3] An emphasis is usually placed on the importance of the back-donation as crucial to H−H bond cleavage. It is assumed that sterics has no effect on the relative stability of η^2-dihydrogen versus dihydride coordination.[2]

In the first decade after discovery of dihydrogen complexes, the prevailing view of H_2 activation could be that expressed by Kubas in 1993: "the reaction coordinate for oxidative addition of H_2 may be rather flat until relatively precipitous cleavage of the H_2" and "...most H_2 complexes can be expected to have short H−H bonds (<0.9 Å)".[4] However, a number of elongated (also called stretched) dihydrogen complexes with r(H−H) > 1 Å have been prepared in the following decade,[2f] and several such species have been structurally characterized by neutron diffraction (the first structure was reported in 1993 for $IrH(H\cdots H)Cl_2(P^iPr_3)_2$).[5] Transition-metal hydrides known today show a continuum of H−H distances with no certain borderline between η^2-dihydrogen and dihydride. It appears, however, that complexes with the H−H distances between 1 and 1.5 Å have some properties which make them different from "genuine" η^2-dihydrogen or dihydride species. One, which may be not widely appreciated, is the flatness of the potential energy surface (PES) along the H···H stretch (or H−M−H bend),[2f,6] possibly making the distance (and all dependent spectroscopic properties) sensitive to sterics, solvation or crystal packing, and weak bonding interactions such as hydrogen bonding. In this regard, the complex $IrH(H\cdots H)Cl_2(P^iPr_3)_2$ is an interesting example. Morris at al. wrote in 1994 that they "wondered whether the H−H distance elongates (from 1.11 Å in the crystal) to about 1.3 Å when this complex dissolves in solution."[7] They suggested that "this might happen because of the breaking of the intermolecular H-bond between the (H···H) unit and a terminal chloride (as seen in Figure 1) which could only exist in the crystal lattice." The authors of the original publication on $IrH(H\cdots H)Cl_2(P^iPr_3)_2$ subsequently agreed that they "could not exclude that in solution the molecule was a C_{2v} iridium(V) trihydride."[8] In this paper, we address the controversy and present results of a DFT computation study of $IrH_3Cl_2(PH_3)_2$ (**1**) and $IrH_3Cl_2(P^iPr_3)_2$ (**2**) complexes.

Results and Discussion

The Simple Model. $IrH_3Cl_2(PH_3)_2$ (**1**) has already been a subject of DFT calculations.[9a] Structure **1a** in Figure 2 is a reconstruction of the optimized geometry from ref 9a and represents a dihydrogen complex with the H−H distance of 0.98 Å. A frequency calculation carried out for **1a** in the present

(1) Kubas, G. J.; Ryan, R. R.; Swanson, B. I.; Vergamini, P. J.; Wasserman, H. J. *J. Am. Chem. Soc.* **1984**, *106*, 451.
(2) (a) Kubas, G. J. *Metal Dihydrogen and σ-Bond Complexes: Structure, Theory and Reactivity*; Kluwer: New York, 2001. (b) *Recent Advances in Hydride Chemistry*; Peruzzini, M., Poli, R., Eds; Elsevier: Amsterdam, 2001. (c) Maseras, F.; Lledós, A.; Clot, E.; Eisenstein, O. *Chem. Rev.* **2000**, *100*, 601. (d) Heinekey, D. M.; Oldham, W. J., Jr. *Chem. Rev.* **1993**, *93*, 913. (e) Jessop, P. G.; Morris, R. H. *Coord. Chem. Rev.* **1992**, *121*, 155. (f) Heinekey, D. M.; Lledós, A.; Lluch, J. M. *Chem. Soc. Rev.* **2004**, *33*, 175.
(3) Kubas, G. J. *J. Organomet. Chem.* **2001**, *635*, 37.
(4) Kubas, G. J.; Burns, C. J.; Eckert, J.; Johnson, S. W.; Larson, A. C.; Vergamini, P. J.; Unkefer, C. J.; Khalsa, G. R. K.; Jackson, S. A.; Eisenstein, O. *J. Am. Chem. Soc.* **1993**, *115*, 569.
(5) (a) Gusev, D. G.; Bakhmutov, V. I.; Grushin, V. V.; Vol'pin, M. E. *Inorg. Chim. Acta* **1990**, *177*, 115. (b) Albinati, A.; Bakhmutov, V. I.; Caulton, K. G.; Clot, E.; Eckert, J.; Eisenstein, O.; Gusev, D. G.; Grushin, V. V.; Hauger, B. E.; Klooster, W. T.; Koetzle, T. F.; McMullan, R. K.; O'Loughlin, T. J.; Pélissier, M.; Ricci, J. S.; Sigalas, M. P.; Vymenits, A. B. *J. Am. Chem. Soc.* **1993**, *115*, 7300.
(6) (a) Esteruelas, M. A.; Lledós, A.; Martin, M.; Maseras, F.; Oses, R.; Ruiz, N.; Tomas, J. *Organometallics* **2001**, *20*, 5297. (b) Barea, G.; Esteruelas, M. A.; Lledós, A.; López, A. M.; Tolosa, J. I. *Inorg. Chem.* **1998**, *37*, 5033. (c) Gelabert, R.; Moreno, M.; Lluch, J. M.; Lledós, A. *J. Am. Chem. Soc.* **1998**, *120*, 8168. (d) Gelabert, R.; Moreno, M.; Lluch, J. M.; Lledós, A. *J. Am. Chem. Soc.* **1997**, *119*, 9840.
(7) Klooster, W. T.; Koetzle, T. F.; Jia, G.; Fong, T. P.; Morris, R. H.; Albinati, A. *J. Am. Chem. Soc.* **1994**, *116*, 7677.
(8) Gusev, D. G.; Kuhlman, R. L.; Renkema, K. B.; Eisenstein, O.; Caulton, K. G. *Inorg. Chem.* **1996**, *35*, 6775.

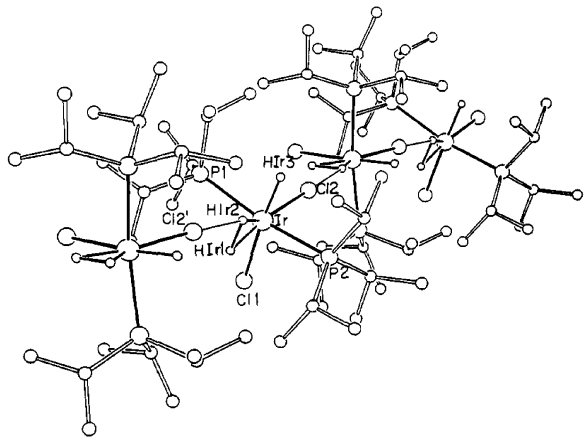

Figure 1. Crystal packing of $IrH(H\cdots H)C1_2(P^iPr_3)_2$ showing intermolecular hydrogen bonding (reproduced from ref 5b).

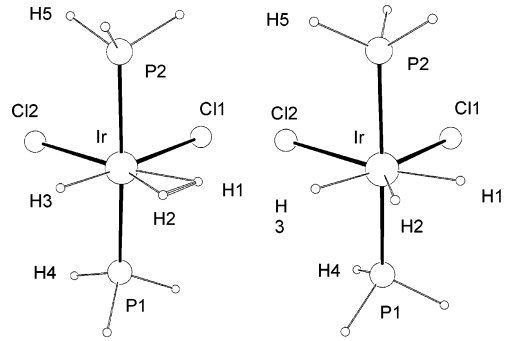

Figure 2. Structures of **1a** (left) and **1b** (right) optimized at the B3LYP/bs1 and *m*PW1PW91/bs2 levels, respectively (the basis sets are explained in the Computational Details).

work gave two imaginary frequencies for PH_3 torsions, and the structure, apparently, is not a stationary point. It could be reproduced only when the dihedral angles Cl2−Ir−P1−H4 and Cl2−Ir−P2−H5 were kept frozen at 0°.[9b] The ground state for $IrH_3Cl_2(PH_3)_2$ is the trihydride **1b**—a minimum lying 1.5 kcal/mol under **1a** (at the B3LYP/bs1 level). Complex **1b** is a C_2 symmetrical molecule with the H1−H2 and H2−H3 distances equal to 1.56 Å. Unlike **1a**, where the PH_3 groups are in an eclipsed conformation, the structure of **1b** possesses staggered phosphines (∠H4−P1−P2−H5 = 84.7°). This is different from the crystal structure of $IrH(H\cdots H)Cl_2(P^iPr_3)_2$ where the P^iPr_3 groups are eclipsed.

The energy plot in Figure 3 shows a single minimum, corresponding to **1b**, on the *m*PW1PW91/bs2 potential energy surface (PES) and no dihydrogen tautomer $IrH(H_2)Cl_2(PH_3)_2$ existing along with it. The plot exhibits a remarkable flatness of the studied cross-section of PES where it takes less than 1 kcal/mol (i.e., less than the zero-point energy of the H−Ir−H bending vibrations, ν = 798, 857 cm^{-1})[10a] to change the H−H distance from 1.56 to 1 Å.[10b] Thus, the consideration of the

(9) (a) Maseras, F.; Lledós, A.; Costas, M.; Poblet, J. M. *Organometallics* **1996**, *15*, 2947. (b) With the two angles activated, B3LYP/bs1 and B3LYP/bs2 optimizations started from **1a** converged to another dihydrogen complex which structure is very similar to **1a**, with the only difference being that two P−H bonds of the eclipsed PH_3 ligands are almost coplanar with Ir−H1, and not with Ir−Cl2. This structure is a minimum lying 0.4 kcal/mol above **1b**. Similar calculations at the B3PW91/bs2 and *m*PW1PW91/bs2 levels, however, both converged to the trihydride structure **1b** and did not find any dihydrogen isomer $IrH(H_2)Cl_2(PH_3)_2$. Regardless of whether the dihydrogen structure is an artifact or a true isomer, the results again demonstrate the flatness of the PES in this system where small perturbations can significantly alter the H−H distance.

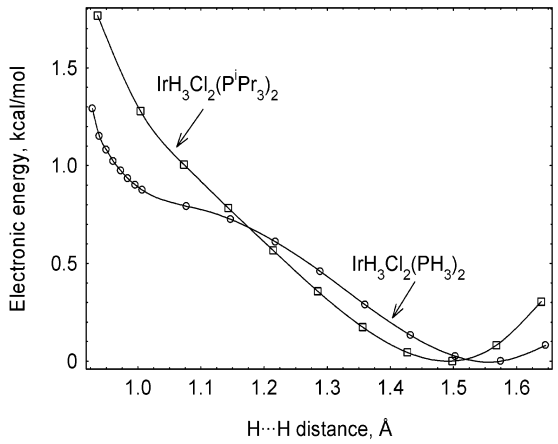

Figure 3. Relaxed *m*PW1PW91/bs2 potential energy scans for $IrH_3Cl_2(PH_3)_2$ and $IrH_3Cl_2(P^iPr_3)_2$ carried out by varying the H1−Ir−H2 angle. The energies are relative to the corresponding minimums.

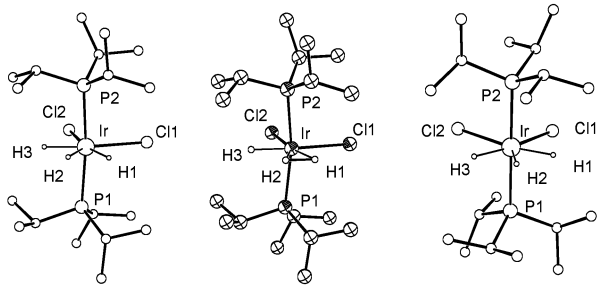

Figure 4. Optimized *m*PW1PW91/Bs2 geometries of **2a** (left), **2b** (right), and the crystal structure of $IrH(H\cdots H)Cl_2(P^iPr_3)_2$ (center).

small model $IrH_3Cl_2(PH_3)_2$ found the ground state different from the crystal structure of $IrH(H\cdots H)Cl_2(P^iPr_3)_2$ and suggested that the H−H distance in this system can be considerably affected by weak interactions.

The "Real" System. This section presents results of calculations for $IrH_3Cl_2(P^iPr_3)_2$ (**2**), a system incorporating relatively bulky and good donor phosphine ligands, P^iPr_3, differing greatly from the small PH_3. It is important to point out that trialkylphoshine−metal complexes can have several conformational or rotational isomers. For example, there are fifteen crystal structures of molecules containing two halide and *trans*-P^iPr_3 ligands in the Cambridge Structural Database, of which nine possess eclipsed phosphines and six have them staggered. The crystal structure of **2** is a natural choice of the starting geometry for optimization of the isomer of $IrH_3Cl_2(P^iPr_3)_2$ possessing eclipsed P^iPr_3 (**2a**). Atomic coordinates of the stretched dihydrogen complex $Re(H\cdots H)(NO)Br_2(P^iPr_3)_2$[11a] were used in this work to develop a model of the staggered structure of $IrH_3Cl_2(P^iPr_3)_2$ (**2b**) by replacing the metal, nitrosyl, and bromide ligands by iridium, hydride, and chloride ligands, respectively. Optimizations of the two models successfully converged to two minimums. Figure 4 shows the calculated **2a** and **2b** alongside the crystal structure of $IrH(H\cdots H)Cl_2(P^iPr_3)_2$, and Figure 3 shows a plot of the electronic energy vs H1−H2 distance in **2a**. Selected distances and angles for the structures in Figure 4 are collected in Table 1.

(10) (a) Scaled vibrational frequencies; scaling factor = 0.957. (b) Similarly, flat PES have been reported for other elongated dihydrogen complexes.[2f,6]

(11) (a) Gusev, D.; Llamazares, A.; Artus, G.; Jacobsen, H.; Berke, H. *Organometallics* **1999**, *18*, 75. (b) Desrosiers, P. J.; Cai, L.; Lin, Z.; Richards, R.; Halpern, J. *J. Am. Chem. Soc.* **1991**, *113*, 4173.

Table 1. Interatomic Distances (Å) and Angles (deg) for the Experimental and Calculated Structures of $IrH_3Cl_2(P^iPr_3)_2$

data	H1–H2	H2–H3	Ir–H1	Ir–H2	Ir–H3	Ir–P	Ir–Cl1	Ir–Cl2	H3–Ir–Cl2	H1–Ir–Cl1	Cl2–Ir–Cl1	P1–Ir–P2
n-diffraction	1.11	1.78	1.55	1.54	1.58	2.362	2.496	2.444	83.3	78.0	87.0	168.5
$IrH_3Cl_2(P^iPr_3)_2$(**2a**)	1.49	1.61	1.58	1.56	1.57	2.387	2.481	2.462	77.7	76.0	87.5	173.5
$IrH_3Cl_2(P^iPr_3)_2$(**2b**)	1.55	1.55	1.57	1.56	1.57	2.385	2.476	2.476	76.4	76.4	88.6	176.6
$[IrH_3Cl_2(P^iPr_3)_2]_2$ molecule B	1.03	1.92	1.62	1.61	1.57	2.387	2.537	2.417	82.7	73.3	92.8	171.2
$[IrH_3Cl_2(P^iPr_3)_2]_2$ molecule A	1.50	1.60	1.57	1.56	1.57	2.389	2.481	2.475	78.0	76.3	87.1	172.2

The optimized **2b** has C_2 symmetry with the rotational axis coinciding with the Ir−H2 bond. This structure is 2.1 kcal/mol lower than the C_s symmetrical **2a**. The two structural forms can coexist in a rapid equilibrium and, given the higher energy, **2a** is probably not the main isomer in solution. The overall H1−Ir−H3 angle in **2a** and **2b** is 118.8−118.5° and is the same as the H1−Ir−H3 angle (118.6°) in **1b** but larger than that in the crystal structure (111.7°). The Cl1−Ir−Cl2 angles are similar in all four structures: 87.8 (**1b**), 87.5 (**2a**), 88.6 (**2b**), and 87° in the crystal. A surprising difference between **1b** and **2a** is the *shorter* H1−H2 distance in the latter, 1.49 Å, as if the system were "fine-tuned" to have more η^2-H_2 character. Considering the higher basicity of P^iPr_3 relative to PH_3, this is unexpected because the more electron-rich metal center in **2a** should favor a trihydride structure. The difference between **1b** and **2a** is most likely due to the coordinated P^iPr_3 which has low local symmetry and is large enough to interfere with the hydrides. Consequently, the environments occupied by H1 and H3 are inequivalent; in particular, there is more repulsion experienced by H2 from the methyl groups wedging between this hydride and its neighbor, H3. This repulsion forces H2 to depart toward H1 and shortens the H1−H2 distance. This explanation is supported by the observation that H1 and H3 are equivalent in the C_2-symmetrical **2b** where H1−H2 = H2−H3 = 1.55 Å. The plot in Figure 3 shows that increasing the H1−H2 distance in **2a** from 1.49 to 1.56 Å would result in the energy rising by 0.065 kcal/mol, as well as reducing this separation from 1.56 to 1.49 Å in **1b** would cost 0.040 kcal/mol, giving an estimate for the repulsion energy as ca. 0.1 kcal/mol.

We have also studied hydride ligand exchange in **2a** and optimized a transition structure **2TS** presented in Figure 5, which

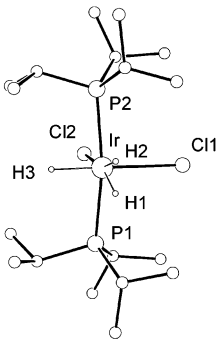

Figure 5. *m*PW1PW91/bs2-optimized geometry of **2TS**. Key distances (Å) and angles (deg): H1−H2 0.95, Ir−H1 1.64, Ir−H2 1.64, Ir−H3 1.57, Ir−Cl2 2.397, Ir−Cl1 2.521, Ir−P1 2.400, Cl1−Ir−Cl2 91.9, H1−Ir−Cl1 88.1, Cl2−Ir−H3 89.5, H1−Ir−H3 90.6, H1−Ir−H2 33.8.

shows the H1−H2 pair rotated by 90°, halfway between the starting and product (H1/H2 exchanged) geometries. The free energy of **2TS** is 3.8 kcal/mol above **2a** at the *m*PW1PW91/bs2 level. A slightly lower and probably more accurate value, $\Delta G^{\ddagger}$ = 3.1 kcal/mol, was calculated at the *m*PW1K/bs2 level. It could be expected that the energy barrier for the hydride exchange in **2a** lies between 2 and 5 kcal/mol. The lower limit was estimated for $IrH(H\cdots H)Cl_2(P^iPr_3)_2$ by inelastic neutron scattering.[5b] The upper limit is likely ca. 5 kcal/mol because no decoalescence of the hydride resonance could be observed in the low temperature ^1H NMR spectra of $IrH_3Cl_2(P^iPr_3)_2$ or $IrHD_2Cl_2(P^iPr_3)_2$. The Arrhenius activation energy for the molecular tumbling of this complex in solution was determined as E_a = 3−3.56 kcal/mol;[5b] thus, the hydride ligand exchange in **2a** is approximately as fast as the molecular reorientation.

The Hydrogen-Bonded System. To investigate the effect of hydrogen bonding on the H−H distance, two *optimized* molecules of **2a** were brought together in an arrangement mimicking the crystal structure in Figure 1, i.e., at the Ir−Ir′ distance of 6.54 Å and rotated to make ∠P1−Ir−Ir′−P1′ = 61.3°. Optimization of this model afforded a dimer shown in Figure 6; selected distances and angles for the structure are

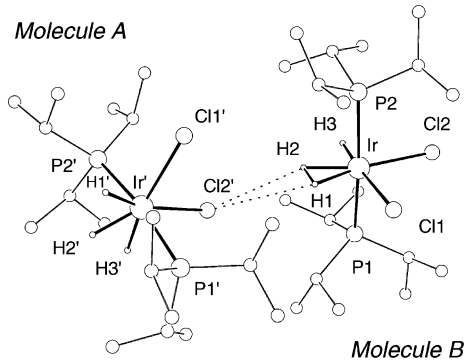

Figure 6. *m*PW1PW91/bs2-optimized geometry of the hydrogen-bonded dimer $[IrH_3Cl_2(P^iPr_3)_2]_2$.

collected in Table 1. During optimization, the two molecules slightly drifted apart and rotated: the Ir−Ir′ distance elongated to 6.68 Å and the P1−Ir−Ir′−P1′ angle increased to 77.4°. Therefore, the Cl2′−H2 and Cl2′−H1 distances are also longer in the model system (3.12 vs 2.64 Å and 3.20 vs 3.04 Å, respectively) and the Ir′−Cl2′ bond in the model is not oriented toward the other metal center as much as in the crystal (∠Ir′−Cl2′−Ir = 139 vs 163°). The differences are probably due to more constrained packing of the molecules in the crystal lattice; nonetheless, the model system possesses some of the important features of the crystal structure.

The optimized molecule A in $[IrH_3Cl_2(P^iPr_3)_2]_2$ remains very similar to **2a**; the differences are limited to (i) an elongation (0.014 Å) of the Ir′−Cl2′ bond as a consequence of the Cl′···H2 and Cl′···H1 hydrogen bonding and (ii) a slightly reduced P1′−Ir′−P2′ angle, 172.2 vs 173.3°. It is molecule B that has undergone a transformation during the optimization, mainly involving the H1−H2 distance which shortened to 1.03 Å.

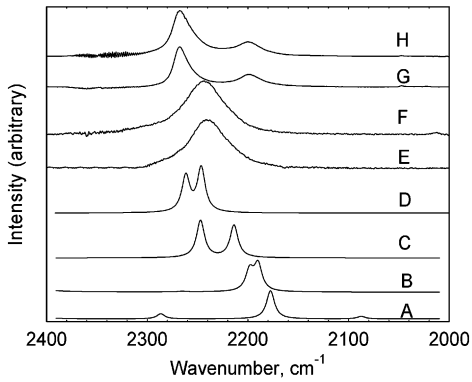

Figure 7. Calculated[10a] (A−D) and experimental (E−H) IR spectra in the Ir−H stretching region: A, $IrH(H_2)Cl_2(PH_3)_2$ (**1a**); B, $IrH_3Cl_2(PH_3)_2$ (**1b**); C, $IrH_3Cl_2(P^iPr_3)_2$ (**2a**); D, $IrH_3Cl_2(P^iPr_3)_2$ (**2b**), E, toluene solution; F, THF solution; G, Nujol mull; H, KBr pellet.

Molecule B is an octahedral dihydrogen complex $IrH(H_2)Cl_2(P^iPr_3)_2$ with distinctly different Ir−Cl bonds: long Ir−Cl1 = 2.537 Å (trans to the hydride) and short Ir−Cl2 = 2.417 Å (trans to the H_2 ligand). The Ir−H1 and Ir−H2 distances lengthened from 1.58 and 1.56 Å in **2a** to 1.62 and 1.61 Å in molecule B, respectively. The Ir−H bonds are surprisingly short in the crystal (1.55(2) and 1.54(2) Å) that may be due to the somewhat poor quality of the structure ($wR(F_o) = 11.9$) which, for example, shows some C−H bonds as short as 0.82−1 Å and several as long as 1.16−1.25 Å. Comparing the experimental geometry and that of molecule B, one should note a good agreement for the H1−Ir−H3, H3−Ir−Cl1, and P1−Ir−P2 angles: 111.7°, 83.3°, and 168.5° vs 111.2°, 82.7°, and 171.2°, respectively. Although the calculated H1−H2 bond is shorter than the experimental (1.03 vs 1.11 Å), the overall agreement is satisfactory within the limits of the model.

Formation of the H_2 ligand is expected to increase the acidity of H1 and H2 and stabilize their hydrogen bonding to Cl2′. That may be the reason a dihydrogen structure is favored by molecule B and in the crystal lattice. It is interesting that $IrH_3Cl_2(P^iPr_3)_2$ eliminates HCl in solution and exists in a rapid equilibrium with the dihydride $IrH_2Cl(PiPr_3)_2$. The PES plot in Figure 3 shows that when H1 and H2 are 1.03 Å close in **2a**, the energy should rise by ca. 1.2 kcal/mol. This is well offset by the energy stabilization of the hydrogen bond that makes the dimer structure 4.1 kcal/mol more stable than two isolated molecules of **2a**.

Experimental Results and Comparison with the Calculated Data. IR spectroscopic data provide strong evidence for different structures of the iridium complex in solution and the solid. Figure 7 shows calculated Ir−H stretching vibrations[10a] in **1a**, **1b**, **2a**, and **2b** and the experimental absorptions of $IrH_3Cl_2(P^iPr_3)_2$ in the solid state (KBr, Nujol mull) and in toluene and THF solutions. For **1a**, all three fundamental vibrations are seen, although one of them, the H−H stretch, can be very broad and difficult to detect in an experimental spectrum. In the trihydrides **1b**, **2a**, and **2b**, the Ir−H2 stretching vibration is very weak, and the two observable absorptions are due to the coupled symmetrical and antisymmetrical H1−Ir−H3 stretching modes. These two have similar intensities and are relatively close (2190/2198 cm^{-1} in **1b**, 2213/2247 cm^{-1} in **2a**, and 2246/2262 cm^{-1} in **2b**), whereas the peak separations are larger in **1a** where the Ir−H3 stretch (2178 cm^{-1}) is far more intense than the other two absorptions (2287, 2087 cm^{-1}).

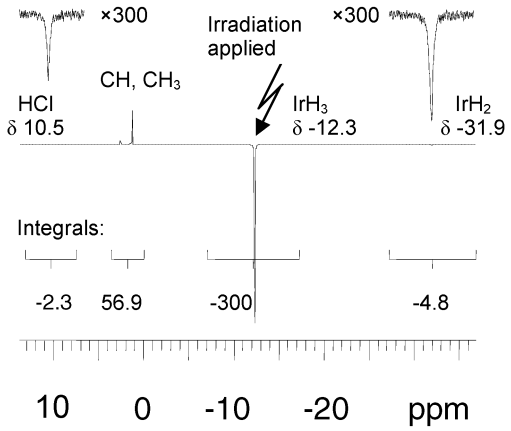

Figure 8. Difference NOE spectrum of $IrH_3Cl_2(P^iPr_3)_2$ obtained by saturating the IrH_3 resonance. (Top) the two insets show inverted resonances of HCl and $IrH_2Cl(P^iPr_3)_2$ arising due to saturation transfer from $IrH_3Cl_2(P^iPr_3)_2$.

Based on the theoretical results, the experimental IR data can be interpreted as follows. The two peaks in the solid-state spectra of $IrH(H\cdots H)Cl_2(P^iPr_3)_2$ are due to Ir−H3 (2268 cm^{-1}) and antisymmetrical H1−Ir−H2 (2200 cm^{-1}) stretching vibrations. In the solution spectra, the single broad band at ca. 2244−2241 cm^{-1} most likely contains overlapped and unresolved symmetrical and antisymmetrical H1−Ir−H3 stretches of the trihydride, $IrH_3Cl_2(P^iPr_3)_2$, as a mixture of rotational isomers analogous to **2a** and **2b**.

In the fingerprint region, the solution IR spectra in toluene, THF, and CH_2Cl_2 are practically the same (ignoring the solvent interference); however they show systematic differences when compared to the solid-state spectra. Three prominent peaks attributable to Ir−H bending vibrations at 526, 824, and 1064 cm^{-1} in the KBr and Nujol samples appear shifted to 593, 800, and 1036 cm^{-1}, respectively, in solution.

Some NMR properties have been already reported for $IrH_3Cl_2(P^iPr_3)_2$ at 200 MHz.[5] In this work, additional data were collected at 300 MHz in three solvents: toluene-d_8, THF-d_8, and CD_2Cl_2. The IrH_3 resonance is broad in the room-temperature ^1H NMR spectra due to the rapid equilibrium, $IrH_3Cl_2(P^iPr_3)_2 \leftrightarrows IrH_2Cl(P^iPr_3)_2 + HCl$, that has been a subject of an earlier study.[5] The line width shows a pronounced solvent dependence: the IrH_3 resonance is extremely broad in THF-d_8 (1516 Hz); it is narrower in toluene-d_8 (172 Hz) and, counterintuitively, the narrowest in CD_2Cl_2 (53 Hz). Also, the IrH_3 resonance is observed as a well-resolved triplet ($^2J_{HP} = 8.0$ Hz) at −20 °C in CD_2Cl_2, whereas in the other two solvents the best resolution is achieved at a lower temperature, −40 °C.

Figure 8 is a difference NOE spectrum of $IrH_3Cl_2(P^iPr_3)_2$ recorded in THF-d_8 at −40 °C that exhibits the proton resonances of HCl and $IrH_2Cl(P^iPr_3)_2$ involved in the exchange. Hydrogen chloride is probably bonded to the solvent molecules, $C_4D_8O\cdot HCl$, in tetrahydrofuran. The equilibrium concentrations of HCl and $IrH_2Cl(P^iPr_3)_2$ are small at −40 °C and become vanishingly small below −40 °C in THF-d_8. Low-temperature ^1H spectra in CD_2Cl_2 and toluene-d_8 do not show detectible HCl and $IrH_2Cl(P^iPr_3)_2$, and the equilibrium must be strongly shifted to the left in these solvents.

Results of the T_1 relaxation time measurements are presented in the plot of Figure 9. In toluene, T_1 goes through a minimum of 56.5 ms at −67 °C, in agreement with $T_{1min} = 57$ ms obtained

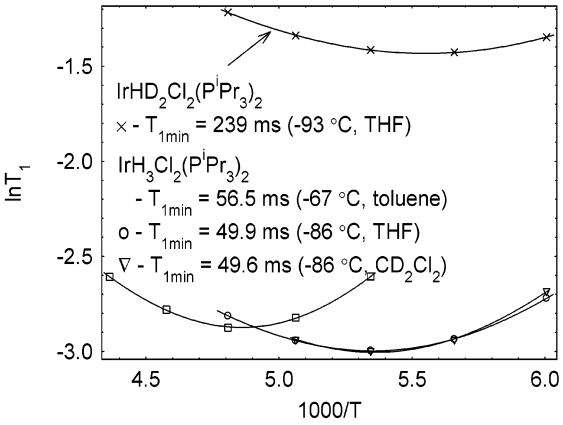

Figure 9. ^{1}H T_1 relaxation data at 300 MHz for $IrH_3Cl_2(P^iPr_3)_2$ and $IrHD_2Cl_2(P^iPr_3)_2$.

by conversion of the 38 ms time previously reported in this solvent for $IrH_3Cl_2(P^iPr_3)_2$ at −83 °C and 200 MHz.[5] The minima are shifted to −86 °C in the less viscous THF and CD_2Cl_2, where T_{1min} are 49.9 and 49.6 ms, respectively, i.e., slightly shorter than the T_{1min} time in toluene. This might be an indication of somewhat shorter H−H distances in $IrH_3Cl_2(P^iPr_3)_2$ in THF and CD_2Cl_2 compared to those in toluene.

The methodology of Halpern and co-workers[11b] allows calculating spin−lattice relaxation rates from distances between the interacting spins. No correction for rapid H_2 spinning is required for **2** because the 2-fold H−H reorientation via **2TS** should have no influence on the T_1.[8,12] This approach afforded calculated T_{1min} = 60.8 s for **2a** and 59.7 ms for **2b** (with the contributions to the relaxation, R* = 3.5−3.9 s^{-1}, from the phosphines and R_{HH} = 12.9−12.8 s^{-1} due to the interactions between the hydrides, all data at 300 MHz), in a close agreement with T_{1min} = 56.5 ms in toluene. The experimental $1/T_{1min}$ relaxation rate of IrH in $IrHD_2Cl_2(P^iPr_3)_2$ is 4.2 s^{-1} in THF-d_8 and is greater than the calculated R* due to the H−D relaxation contribution, R_{HD}. The latter is $0.063R_{HH}$,[11b] i.e., the experimental R* = 3.1 s^{-1} (R_{HH} = 16.9 s^{-1}) in THF.

The experimental T_{1min} = 56.5 ms time in toluene would be reproduced exactly if the H1−H2 and H2−H3 distances were 1.42 and 1.68 Å, respectively, in a C_s-symmetrical structure like **2a** (keeping ∠H1−Ir−H3 = 118.3°), or if H1−H2 and H2−H3 were both at 1.51 Å in a C_2-symmetrical structure like **2b**. It is important to emphasize, however, that the theoretical and experimental distances *should not be the same*. The H−H distances in **2a** and **2b** correspond to their minimums on the PES. The experimental distances are *vibrationally averaged* and could have matched the theoretical values only if the vibrations had been harmonic. In reality, the hydride vibrations are anharmonic,[6] and the effective distances can be longer or shorter depending on the shape of the PES. It is normally expected that in a vibrating diatomic fragment A−B the energy raises on shortening the distance more than when the A−B bond is stretched. Hence, the vibrationally averaged r(A−B) would normally to be slightly longer than the distance corresponding to the electronic energy minimum. A different situation can be found in a compressed dihydride complex where the energy may rise more steeply on elongating rather than on shortening

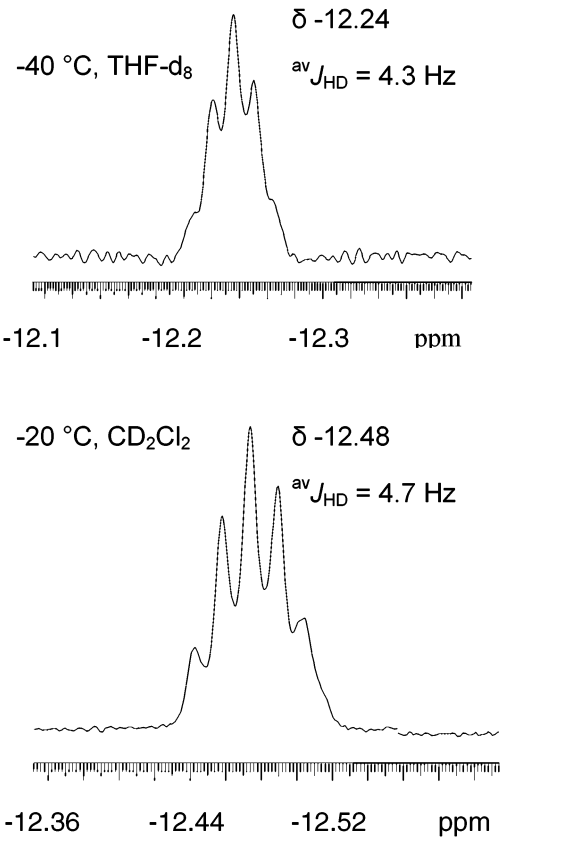

Figure 10. $^1H\{^{31}P\}$ NMR spectra of $IrHD_2Cl_2(P^iPr_3)_2$ in THF-d_8 and CD_2Cl_2 (resolution enhancement was applied to better resolve the splitting of the lines). The chemical shifts of IrH_3 are −12.29 (−40°) and −12.55 ppm (−20°) in the two solvents, respectively.

of the H−H distance, thus resulting in an effective distance shorter than the one obtained by energy minimization in a DFT calculation. This behavior has been recently documented for the compressed dihydride $[IrH_2Cp^*(dmpm)]^{2+}$.[13a]

The H−D coupling, $^{av}J_{HD}$, could not be resolved in the earlier study of $IrDH_2Cl_2(P^iPr_3)_2$ and $IrD_2HCl_2(P^iPr_3)_2$; however, the spectra simulations suggested an estimate of $^{av}J_{HD} = 4 \pm 1$ Hz.[5b] We prepared solutions of $IrHD_2Cl_2(P^iPr_3)_2$ in THF-d_8 and CD_2Cl_2 and recorded the $^1H\{^{31}P\}$ NMR spectra shown in Figure 10 that indeed revealed H−D couplings of 4.3 and 4.7 Hz, respectively. The smaller coupling in THF is probably underestimated due to more broadening of the resonance, which is poorly resolved.

Theoretically, $^{av}J_{HD}$ in a three-spin system is an average of the three couplings, $^{av}J_{HD} = {}^1/_3\{J_{HD}(1-2) + J_{HD}(2-3) + J_{HD}(1-3)\}$. These cannot be measured for $IrHD_2Cl_2(P^iPr_3)_2$ because of the rapid H/D site exchange, and there is no reliable empirical correlation between J_{HD} and r(H−H) for long H−H distances such as in **2a** and **2b**. Experimental and theoretical data collected in the Appendix give compelling evidence that $J_{HD}(1-2)$ and $J_{HD}(2-3)$ in **2a** and **2b** can be predicted by DFT calculations followed by corrections using eq 4 (see the Appendix for details). For example, for the related iridium trihydride $[IrH_3Cp(PMe_3)]^+$ (where r(H−H) = 1.69 Å), the

(12) (a) Zilm, K. W.; Millar, J. M. *Adv. Magn. Opt. Reson.* **1990**, *15*, 163. (b) Facey, G. A.; Fong, T. P.; Gusev, D.; Macdonald, P. M.; Morris, R. H.; Schlaf, M.; Xu, W. *Can. J. Chem.* **1999**, *77*, 1899.

(13) (a) Gelabert, R.; Moreno, M.; Lluch, J. M.; Lledós, A.; Pons, V.; Heinekey, D. M. *J. Am. Chem. Soc.* **2004**, *126*, 8813. (b) Heinekey, D. M.; Millar, J. M.; Koetzle, T. F.; Payne, N. G.; Zilm, K. W. *J. Am. Chem. Soc.* **1990**, *112*, 909. (c) Heinekey, D. M.; Hinkle, A. S.; Close, J. D. *J. Am. Chem. Soc.* **1996**, *118*, 5353. (d) Pons, V.; Heinekey, D. M. *J. Am. Chem. Soc.* **2003**, *125*, 8428.

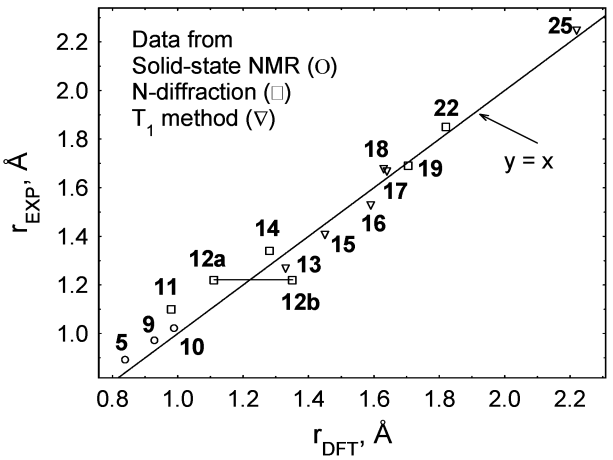

Figure 11. Experimental and calculated H−H distances in dihydrogen and dihydride complexes (data from Table 2, Appendix).

corrected theoretical coupling $J_{HD}(1-2) = J_{HD}(2-3) = 3.6$ Hz compares well to the experimental value, 3.9 Hz.[13b,c] In another iridium complex, $[IrH_2Cp^*(dmpm)]^{2+}$, where $r(H-H) = 1.53$ Å, the corrected theoretical coupling $J_{HD} = 7.1$ Hz is at the lower end of the experimental temperature-dependent $J_{HD} = 7.3$ (−50 °C) − 9.0 Hz (20 °C).[13a,d] This approach afforded $J_{HD}(1-2)$ and $J_{HD}(2-3)$ couplings in **2a**: 12.6 Hz for $r(H1-H2) = 1.49$ Å and 5.2 Hz for $r(H2-H3) = 1.61$ Å, respectively. In **2b**, the two couplings are the same: $J_{HD}(1-2) = J_{HD}(2-3) = 7.1$ Hz for $r(H-H) = 1.55$ Å. If $J_{HD}(1-3) \approx 0$ Hz (that seems appropriate when $r(H-H) \approx 2.7$ Å; see the data in Table 2 in the Appendix),[14a] then $^{av}J_{HD}(calc) = 5.9$ Hz in **2a** and 4.7 Hz in **2b**. The latter value is in agreement with the experiment.[14b]

Other Dihydrogen Complexes. An interested reader may ask whether $IrH_3Cl_2(P^iPr_3)_2$ is a special case or shows behavior that can be found with other dihydrogen complexes? To answer this question, selected reference data from Table 2 in the Appendix have been collected in Figure 11, which is a plot of experimental vs theoretical distances for a group of representative classical and nonclassical hydrides. For the majority of species in Figure 11 there is a good agreement between the experimental and theoretical distances, with the differences within 0.05 Å. There are, however, larger discrepancies for two stretched dihydrogen complexes $[Ru(H\cdots H)Cp^*(dppm)]^+$ (**11**) and $[Os(H\cdots H)Cl(dppe)_2]PF_6$ (**12a**) that we would like to address.

The experimental H−H distance, 1.10 Å, in **11** is significantly longer than the one calculated by DFT, 0.98 Å. This difference is somewhat surprising considering that the H−D coupling in **11** (21.1−22.3 Hz) is practically the same as that (22.1 Hz) in the closely related complex $[Ru(H_2)Cp(dmpe)]^+$ (**10**), where the experimental H−H distance is 1.02 Å and is matched by the calculated one of 0.99 Å (see Table 2 for details). Complex **11** was previously modeled as $[Ru(H\cdots H)Cp(H_2PCH_2PH_2)]^+$, and the authors successfully argued that the experimental H−H distance can be long due to anharmonic H−H and Ru−H_2 stretching vibrations.[6d] Considering this, it should be noted that the practice of correcting the H−H distances in neutron diffraction studies may result in overestimated distances when only the effect of H_2 librations is considered and that of the H−H and Ru−H_2 stretching vibrations is ignored. The raw crystallographic H−H distance in **11** is 1.08 Å which is still 0.1 Å longer than the theoretical distance, possibly indicating domination of the effect of H−H and Ru−H_2 stretching. The H−H distance in **10** (1.02 Å) has been obtained by solid-state NMR and is believed to be not affected by the vibrations; this can explain a good agreement with the result of the DFT geometry optimization.

Another special case is the stretched dihydrogen complex $[Os(H\cdots H)Cl(dppe)_2]PF_6$ which crystal structure in Figure 12 shows ion-pairing and relatively short H···F contacts: H1−F1 = 2.68 Å and H2−F1 = 2.72 Å. A DFT geometry optimization of this system with a frozen Os−P5 distance converged to geometry **12a** in Figure 12, retaining most of the features of the crystal structure, except that the H−F distances shortened to H1−F1 = 2.33 Å and H2−F1 = 2.38 Å due to a relocation of the $[PF_6]^-$ ion (despite it retaining the crystallographic Os−P5 distance, 5.43 Å). The calculated H−H distance, 1.11 Å, is close to the raw neutron diffraction value of 1.15 Å, whereas the corrected crystallographic H−H distance is longer, 1.22 Å.

When a new DFT calculation was started from the *optimized* **12a** with the $[PF_6]^-$ ion removed from the model, it converged to another minimum (verified by a frequency calculation) of a substantially different geometry **12b** (Figure 12), where the H1−H2 distance increased to 1.35 Å and the hydrogens rotated toward the Cl−P2−P4 plane so that the H1−H2 vector is at 21.4° to this plane in **12b** compared to 62.7° in **12a**. The computational results suggest that the crystal structure of $[Os(H\cdots H)Cl(dppe)_2]PF_6$ would not be the ground-state structure of the metal complex cation in the absence of ion-pairing. One practical implication of this is that the solution structure and NMR properties, T_1 and J_{HD}, of the Os(H···H) unit can be different with $[PF_6]^-$ and with a bulkier nonhalogen based anion, e.g., $[BPh_4]^-$. The $[PF_6]^-$ salt may also show temperature-dependent NMR properties if there is an equilibrium between the ion-paired and dissociated forms of $[Os(H\cdots H)Cl(dppe)_2]PF_6$ in solution. Interestingly, it has been recently shown that ion-pairing in a related system, $[FeH(H_2)(dppe)_2]BF_4$, has a large effect on the rate of deprotonation of this complex.[15]

Experimental Section

All NMR spectra have been obtained with a Varian Unity Inova 300 NMR spectrometer. All chemicals were purchased from Aldrich and Pressure Chemicals and used as received. The solvents, THF-d_8 and toluene-d_8 were dried with Na/K alloy, whereas anhydrous CD_2Cl_2 was vacuum-transferred from P_2O_5. The monohydride and trihydride iridium complexes were prepared following modified versions of the procedures developed by Grushin.[5b,16]

$IrHCl_2(P^iPr_3)_2$. Triisopropylphosphine (0.83 g, 5.2 mmol) was added to $IrCl_3 \cdot nH_2O$ (52% Ir, 0.63 g, 1.7 mmol) in 10 mL of anhydrous 2-propanol. The resulting suspension was refluxed for 21 h under argon and then left at room temperature for 2 h. The dark-purple crystalline product was filtered off, washed with 4 × 3 mL of 2-propanol, and dried under vacuum for 4 h. Yield: 0.78 g (78%). The spectroscopic

(14) (a) $^2J_{HH}(1-3) = \pm 3.4$ Hz in IrH_3Cp^*(*n*-decyl-P(H)Ph) and the H−D coupling $^2J_{HD}(1-3)$ is expected to be ca. ±0.5 Hz.[13b] Our DFT calculations for $^2J_{HD}(1-3)$ gave a small value of +0.2 Hz for **2a** but an unexpectedly large coupling of +5.0 Hz for **2b**. The reason for the difference is unclear; however, the latter value does not make sense. (b) In these calculations we have assumed the same probability for H and D to occupy any of the three sites that might not generally be true.

(15) Basallote, M. G.; Besora, M.; Durán, J.; Fernández-Trujillo, M. J.; Lledós, A.; Máñez, M. A.; Maseras, F. *J. Am. Chem. Soc.* **2004**, *126*, 2320.

(16) Simpson, R. D.; Marshall, W. J.; Farischon, A. A.; Roe, D. C.; Grushin, V. V. *Inorg. Chem.* **1999**, *38*, 4171.

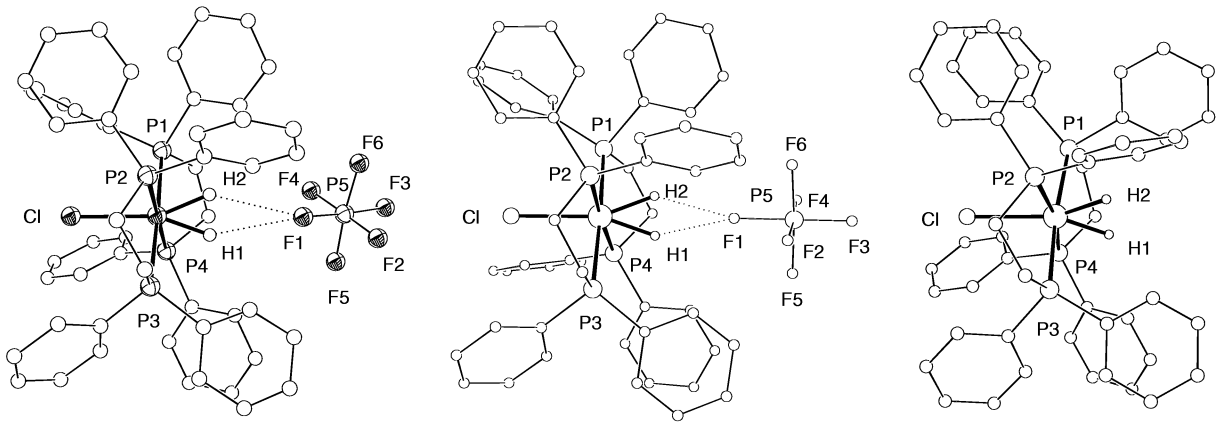

Figure 12. Experimental (left) and theoretical structures of $[Os(H\cdots H)Cl(dppe)_2]PF_6$ (**12a**, center) and $[Os(H\cdots H)Cl(dppe)_2]^+$ (**12b**, right).

properties of the isolated complex were identical with those published for $IrHCl_2(P^iPr_3)_2$.[16]

$IrH_3Cl_2(P^iPr_3)_2$. A solution of $IrHCl_2(P^iPr_3)_2$ (0.66 g, 1.13 mmol) in 10 mL of toluene in a 50 mL Schlenk flask filled with hydrogen and stoppered with a septum was stirred at 75 °C for 1.5 h. Then stirring was discontinued and the flask was left at room temperature for 4 days. Hydrogen consumed in this reaction was supplied via the sidearm of the flask under pressure slightly exceeding 1 atm. The product crystallized in the form of relatively large pale-yellow crystals. After removal of the mother liquor with a pipet, the solid was washed with 4×1.5 mL of hexane and dried under vacuum overnight. Yield: 0.41 g (62%). ^{1}H NMR (toluene-d_8): δ 2.47 (m, 6H, C*H*), 1.09 (dvt, $^3J_{HH}$ = 6.9 Hz, $^vJ_{HP}$ = 7.2 Hz, 36H, CH_3), −12.82 (broad line, line width = 172 Hz, 3H, IrH_3). ^{31}P{^{1}H} NMR (toluene-d_8): δ 25.1 (broad line, line width = 91 Hz).

Preparation of $IrHD_2Cl_2(P^iPr_3)_2$. This complex was prepared by saturating solutions of $IrH_3Cl_2(P^iPr_3)_2$ in THF-d_8 and CD_2Cl_2 with D_2 gas in flame-dried J. Young NMR tubes.

Relaxation times measured in this work. $IrHD_2Cl_2(P^iPr_3)_2$ (THF-d_8): T_1 = 296 (−65 °C), 262 (−75.5 °C), 243 (−85.9 °C), 240 (−96.3 °C), 260 ms (−106.5 °C). $IrH_3Cl_2(P^iPr_3)_2$ (THF-d_8): T_1 = 60.0 (−65 °C), 52.7 (−75.5 °C), 50.0 (−85.9 °C), 53.1 (−96.3 °C), 65.9 ms (−106.5 °C). $IrH_3Cl_2(P^iPr_3)_2$ (CD_2Cl_2): T_1 = 52.9 (−75.5 °C), 49.9 (−85.9 °C), 52.9 (−96.3 °C), 68.3 ms (−106.5 °C). $IrH_3Cl_2(P^iPr_3)_2$ (toluene-d_8): T_1 = 73.7 (−43.8 °C), 62.0 (−54.5 °C), 56.4 (−65 °C), 59.4 (−75.5 °C), 73.8 ms (−85.9 °C).

Computational Details. The calculations were done with Gaussian 03 (Revision B05) and GaussView (version 3.09) programs.[17] All geometries were fully optimized without symmetry or internal coordinate constraints using the MPW1PW91 functional which included modified Perdew−Wang exchange and Perdew−Wang 91 correlation.[18] The following basis sets were employed in this work: bs1 included LANL2DZ+ECP for Ir, 6-31g(d,p) for all metal-bonded atoms and 6-31g for hydrogens bonded to phosphorus; bs2 included SDD (associated with ECP) for Ir, 6-31g(d, p) for all metal-bonded atoms and 6-31g for all other atoms.[19] The synchronous transit-guided quasi-newton (STQN) method[20a] QST2 was used for the optimization of the transition state **2TS** at the *m*PW1PW91/bs2 level. The nature of the stationary points **1b**, **2a**, **2b**, and **2TS** was verified by frequency calculations; however, no such calculation could be done for the dimer $[IrH_3Cl_2(P^iPr_3)_2]_2$ due to the large size of the system. Geometry optimizations and frequency calculations for **2TS** and **2a** have also been carried out at the *m*PW1K/bs2 level.[21] A method implemented in Gaussian 03 was used for the spin−spin coupling calculations.[20b−d]

Conclusions

The results of DFT calculations and experimental data reported in this paper suggest that in solution $IrH_3Cl_2(P^iPr_3)_2$ is a "compressed" trihydride with relatively short H···H distances. The solid-state dihydrogen structure, where the H1−H2 distance is 1.11(2) Å, may be different from the solution structure mainly due to the weak intermolecular Ir−Cl···H−Ir hydrogen bonding in the crystal lattice. This work demonstrates that the H−H distances in stretched dihydrogen (and compressed dihydride) complexes can be very sensitive to weak intra- and intermolecular interactions, including those with bulky ligands and solvent molecules, hydrogen-bonding interactions, or ion-pairing. For theoretical calculations on such systems, the use of adequate models closely accounting for all structural properties of the "real" systems is very important for accurate geometry and property predictions.

Appendix: H−H Distances and J_{HD} Coupling Constants in Metal Hydrides

A linear correlation between the H−H distance and J_{HD} coupling in dihydrogen complexes has been proposed by Heinekey[22a] and Morris[22b] and co-workers. An equation

(17) Frisch, M. J.; Trucks, G. W.; Schlegel, H. B.; Scuseria, G. E.; Robb, M. A.; Cheeseman, J. R.; Zakrzewski, V. G.; Montgomery, Jr., J. A.; Stratmann, R. E.; Burant, J. C.; Dapprich, S.; Millam, J. M.; Daniels, A. D.; Kudin, K. N.; Strain, M. C.; Farkas, O.; Tomasi, J.; Barone, V.; Cossi, M.; Cammi, R.; Mennucci, B.; Pomelli, C.; Adamo, C.; Clifford, S.; Ochterski, J.; Petersson, G. A.; Ayala, P. Y.; Cui, Q.; Morokuma, K.; Salvador, P.; Dannenberg, J. J.; Malick, D. K.; Rabuck, A. D.; Raghavachari, K.; Foresman, J. B.; Cioslowski, J.; Ortiz, J. V.; Baboul, A. G.; Stefanov, B. B.; Liu, G.; Liashenko, A.; Piskorz, P.; Komaromi, I.; Gomperts, R.; Martin, R. L.; Fox, D. J.; Keith, T.; Al-Laham, M. A.; Peng, C. Y.; Nanayakkara, A.; Challacombe, M.; Gill, P. M. W.; Johnson, B.; Chen, W.; Wong, M. W.; Andres, J. L.; Gonzalez, C.; Head-Gordon, M. E.; Replogle, S.; Pople, J. A. Gaussian, Inc., Pittsburgh, PA, 2001.

(18) (a) Adamo, C.; Barone V. *J. Chem. Phys.* **1998**, *108*, 664. (b) Perdew, J. P.; Burke, K.; Wang, Y. *Phys. Rev. B* **1996**, *54*, 16533. (c) Burke K.; Perdew, J. P.; Wang, Y. In *Electronic Density Functional Theory: Recent Progress and New Directions*; Dobson, J. F., Vignale, G., Das, M. P., Eds.; Plenum: New York, 1998.

(19) For more information about basis sets implemented in Gaussian 03 and references, see: Frish, A.; Frish, M. J.; Trucks, G. W. *Gaussian 03 User's Reference*; Gaussian, Inc.: Pittsburgh, PA, 2003. The basis sets are also available from the Extensible Computational Chemistry Environment Basis Set Database, which is developed and distributed by the Molecular Science Computing Facility, Environmental and Molecular Sciences Laboratory, which is part of the Pacific Northwest Laboratory, P.O. Box 999, Richland, WA 99352 (www.emsl.pnl.gov/forms/basisform.html).

(20) (a) Peng, C.; Ayala, P. Y.; Schlegel, H. B.; Frisch, M. J. *J. Comput. Chem.* **1996**, *17*, 49. (b) Helgaker, T.; Watson, M.; Handy, N. C. *J. Chem. Phys.* **2000**, *113*, 9402. (c) Sychrovsky, V.; Grafenstein, J.; Cremer, D. *J. Chem. Phys.* **2000**, *113*, 3530. (d) Barone, V.; Peralta, J. E.; Contreras, R. H.; Snyder, J. P. *J. Phys. Chem. A* **2002**, *106*, 5607.

(21) (a) Lynch, B. J.; Fast, P. L.; Harris, M.; Truhlar, D. G. *J. Phys. Chem. A* **2000**, *104*, 4811. (b) Zhao, Y.; Pu, J.; Lynch, B. J.; Truhlar, D. G. *Phys. Chem. Chem. Phys.* **2004**, *6*, 673.

Table 2. Experimental and Calculated J_{HD} (Hz) and r(H−H) (Å) Data for Dihydrogen and Hydride Complexes[a]

complex	r(H–H)	J_{HD}
$Cr(H_2)(CO)_3(PPr^i_3)_2$ (**3**)	0.85 (NMR)[24]	(+)35[24]
$Mo(H_2)(CO)(dppe)_2$ (**4**)	0.88 (NMR)[12a]	(+)34[25]
$W(H_2)(CO)_3(PPr^i_3)_2$ (**5**)	0.89 (NMR)[12a]	(+)34[8, 26]
	0.84 (DFT)	*+34.8*
$[Fe(H_2)H(dppe)_2]BPh_4$ (**6**)	0.82−0.85(2) (n-diff)[27]	(+)32 ± 1[27]
	0.90(1)[27a] (NMR)	
$[Ru(H_2)H(dppe)_2]BPh_4$ (**7**)	0.82−0.94(3) (n-diff)[27c]	(+)32−32.5[27c]
$[Ir(H_2)H(bq)(PPh_3)_2]^+$ (**8**)	0.94 (NMR)[12a]	(+)29.5[28]
$[Ru(H_2)Cp(CO)(PCy_3)]^+$ (**9**)	0.97 (NMR)[12a]	(+)28.5[29]
	0.93 (DFT)	*+27.2*
$[Ru(H_2)Cp(dmpe)]^+$ (**10**)	1.02 (NMR)[12a]	(+)22.1[29]
	0.99 (DFT)	*+24.6*
$[Ru(H_2)Cp^*(dppm)]BF_4$ (**11**)	1.08−1.10(3) (n-diff)[7]	(+)21.1−22.3[7]
	0.98 (DFT)	*+25.2*
$[Os(H_2)Cl(dppe)_2]PF_6$ (**12a**)	1.15−1.22(3) (n-diff)[22b]	(+)13.9[22b]
$[Os(H_2)Cl(dppe)_2]^+$ (**12b**)	*1.11* (**12a**) (DFT)	*+9.4* (**12b**)
	1.35 (**12b**) (DFT)	
$Re(H_2)Br_2(NO)(PPr^i_3)_2$ (**13**)	1.27 (T_1)[11a]	(+)12.8[11a]
	1.33 (DFT)	*+9.8*
$[Os(H_2)(en)_2(OAc)]PF_6$ (**14**)	1.34(2) (n-diff)[30]	(+)9[30]
	1.28 (DFT)	*+6.8*
$Os(H_2)Cl(NH{=}C(Ph)C_6H_4)(P^iPr_3)_2$ (**15**)	1.41 (T_1)[31]	(+)6.3[31]
	1.45 (DFT)	*+4.5*
$[IrH_2Cp^*(dmpm)]\{B(C_6F_5)_4\}_2$ (**16**)	1.53 (T_1)[32a]	(+)9.0−7.3[13a,d, 32b]
	1.59 (DFT)	*+5.2*
$[TaH_2Cp_2(P(OMe)_3)]PF_6$ (**17**)	1.67 (T_1)[33]	+1.5[33]
	1.64 (DFT)	+0.4
$OsH_2Cl[CH(C_2H_4P^tBu_2)_2]$ (**18**)	1.57(3) (X-ray)[34]	0[34]
	1.68 (T_1)[34]	*−0.1*
	1.63 (DFT)	
$[IrH_3Cp(PMe_3)]BF_4$ (**19**)	1.69(1) (n-diff)[13b]	+3.9[13c]
	1.705 (DFT)	*+2.4*
$[IrH_3Cp^*(PMe_3)]BF_4$ (**20**)	1.73[13c]	+3.3
	1.74 (DFT)	*+2.0*
NbH_3Cp_2 (**21**)	1.76(9) (X-ray)[36]	−0.9[35]
	1.76 (DFT)	*−1.1*
TaH_3Cp_2 (**22**)	1.85(1) (n-diff)[36]	(−)1.5[35]
	1.82 (DFT)	*−2.0*
$OsH_3(NO)(PPh_3)_2$ (**23**)	2.02(5) (T_1)[37]	(−)0.8[37]
$OsH_3(NO)(PMe_3)_2$ (**24**)	*2.01* (DFT)	*−1.2*
$ReH_2(CO)(NO)(PMe_3)_2$ (**25**)	2.25(15) (T_1)[39]	(−)1.0[38]
	2.22 (DFT)	*−1.0*
$TaH_2Cp_2(BO_2C_6H_4)$ (**26**)	2.3(2) (X-ray)[40]	(−)0.9[40]
	2.03 (DFT)	*−1.2*
$IrH_2Cl(PPhMe_2)(P^iPr_3)_2$ (**27**)	2.53 (X-ray)[41]	(−)0.9[41]
$[IrH_3Cp(PMe_3)]BF_4$ (**19**)	2.66(1) (n-diff)[13b]	N/A
	2.71 (DFT)	*−0.1*
$[IrH_3Cp^*(PMe_3)]BF_4$ (**20**)	*2.76* (DFT)	*+0.4*
$RuH_2(\eta^4\text{-}HSiMe_2(CH{=}CHMe))(PCy_3)_2$ (**28**)	2.8(2) (X-ray)[42]	(−)1.3[42]
NbH_3Cp_2 (**21**)	3.04(9) (X-ray)[36]	N/A
	3.03 (DFT)	*−1.8*
TaH_3Cp_2 (**22**)	3.16(1) (n-diff)[36]	N/A
	3.10 (DFT)	*−1.7*
$OsH_3(NO)(PMe_3)_2$ (**24**)	*3.20* (DFT)	*−1.9*
Trans-FeH_2(*meso*-tetraphos) (**29**)	3.2	(−)2.8[43]

[a] In the absence of experimental information, the couplings which are believed to be negative or positive are given with the signs in parentheses, (−) or (+), respectively. *Italicized* values are from DFT calculations (full computational details are given in the Supporting Information). The distances have been obtained by neutron diffraction (n-diff), X-ray diffraction (X-ray), solid-state ^{1}H NMR (NMR), ^{1}H T_1 method (T_1), or *m*PW1PW91 calculations (DFT). For distances determined by n-diffraction, both the raw value and the value after librational correction are given.

appropriate for relatively short H−H distances, r(H−H) = 1.42 − 0.0167J_{HD} (eq 1),[22b] has been often used in the literature in order to calculate r(H−H) from J_{HD}. Another empirical correlation has been proposed on some theoretical grounds, describing J_{HD} as a function of r(H−H) in the form $J_{HD} = 43\exp((0.74 - r(\text{H}-\text{H}))/0.404) - 2.8(1 - \exp((0.74 - r(\text{H}-\text{H}))/0.404))^2$ (eq 2) for all possible H−H distances, from 0.74 Å in free H_2 to ca. 3.2 Å in *trans*-dihydrides.[22c] A modified version of this correlation has appeared recently as J_{HD} =

(22) (a) Heinekey, D. M.; Luther, T. A. *Inorg. Chem.* **1996**, *35*, 4396. (b) Maltby, P. A.; Schlaf, M.; Steinbeck, M.; Lough, A. J.; Morris, R. H.; Klooster, W. T.; Koetzle, T. F.; Srivastava, R. C. *J. Am. Chem. Soc.* **1996**, *118*, 5396. (c) Gründemann, S.; Limbach, H.-H.; Buntkowsky, G.; Sabo-Etienne, S.; Chaudret, B. *J. Phys. Chem. A* **1999**, *103*, 4752.

(23) Bacskay, G. B.; Bytheway, I.; Hush, N. S. *J. Am. Chem. Soc.* **1996**, *118*, 3753.

(24) Kubas, G. J.; Nelson, J. E.; Bryan, J. C.; Eckert, J.; Wisniewski, L.; Zilm, K. *Inorg. Chem.* **1994**, *33*, 2954.

(25) Kubas, G. J.; Burns, C. J.; Eckert, J.; Johnson, S. W.; Larson, A. C.; Vergamini, P. J.; Unkefer, C. J.; Khalsa, G. R. K.; Jackson, S. A.; Eisenstein, O. *J. Am. Chem. Soc.* **1993**, *115*, 569.

(26) Kubas, G. J.; Unkefer, C. J.; Swanson, B. I.; Fukushima, E. *J. Am. Chem. Soc.* **1986**, *108*, 7000.

(27) (a) Morris, R. H. *Can. J. Chem.* **1996**, *74*, 1907. (b) Ricci, J. S.; Koetzle, T. F.; Bautista, M. T.; Hofstede, T. M.; Morris, R. H.; Sawyer, J. F. *J. Am. Chem. Soc.* **1989**, *111*, 8823. (c) Albinati, A.; Klooster, W. T.; Koetzle, T. F.; Fortin, J. B.; Ricci, J. S.; Eckert, J.; Fong, T. P.; Lough, A. J.; Morris, R. H.; Golombek, A. *Inorg. Chim. Acta* **1997**, *259*, 351.

(28) Crabtree, R. H.; Lavin, M.; Bonneviot, L. *J. Am. Chem. Soc.* **1986**, *108*, 4032.

(29) Chinn, M. S.; Heinekey, D. M. *J. Am. Chem. Soc.* **1990**, *112*, 5166.

(30) Hasegawa, T.; Li, Z.; Parkin, S.; Hope, H.; McMullan, R. K.; Koetzle, T. F.; Taube, H. *J. Am. Chem. Soc.* **1994**, *116*, 4352.

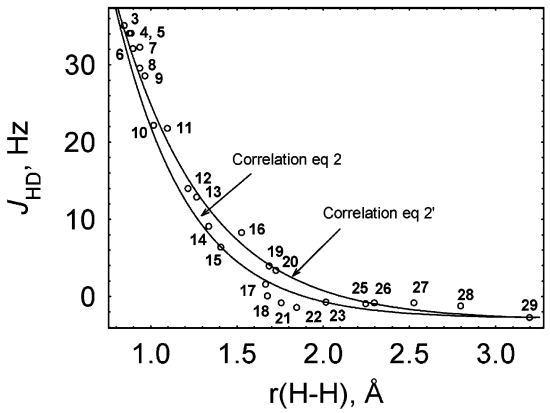

Figure 13. Plots of eqs 2 and 2′ and experimental r(H−H) vs J_{HD} data from Table 2.

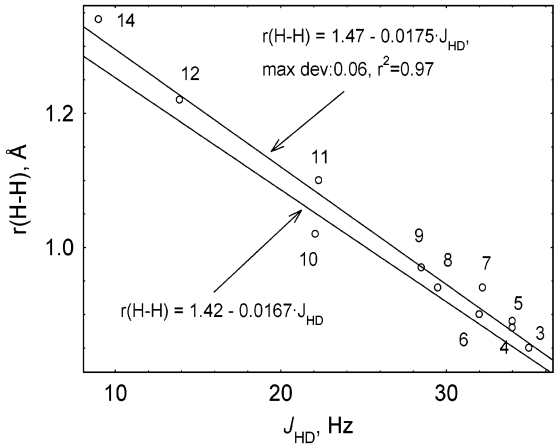

Figure 14. Results of data fitting in the range of H···H distances between 1.34 and 0.85 Å obtained by neutron diffraction and solid-state NMR. Data points (r(H−H), Å/J_{HD}, Hz): 0.85/35 (**3**), 0.88/34 (**4**), 0.89/34 (**5**), 0.90/32 (**6**), 0.94/32.2 (**7**), 0.94/29.5 (**8**), 0.97/28.5 (**9**), 1.02/22.1 (**10**), 1.10/22.3 (**11**), 1.22/13.9 (**12**), 1.34/9.0 (**14**).

43 exp((0.74 − r(H−H))/0.494) − 3.04(1 − exp((0.74 − r(H−H))/0.494))^2 (eq 2′).[13a]

Values of r(H−H) and J_{HD} for representative hydride and dihydrogen complexes are collected in Table 2 and are plotted in Figure 13 together with the plots of eqs 2 and 2′. Figure 14 shows that a linear equation r(H−H) = 1.47 − 0.0175J_{HD}

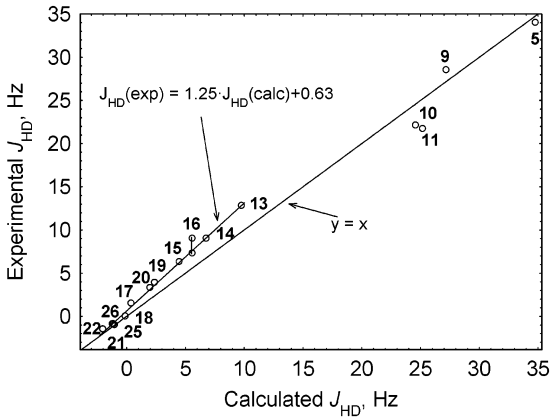

Figure 15. Experimental vs calculated J_{HD} and the result of data fitting for the points between +12.8 and −2 Hz (in the range of H···H distances between 1.27 and 2.3 Å).

(eq 3) fits the data points between 0.85 and 1.34 Å somewhat better than eq 1. It is evident from Figures 13 and 14 that when r(H−H) > 1.3 Å, none of the above correlations is reliable for the purpose of deriving r(H−H) from J_{HD} because of the significant data scatter. For example, in terms of eq 2′, the H−D couplings in complexes **18** (0 Hz), **17** (1.5 Hz), and **19** (3.9 Hz) are associated with the distances as different as 2.11, 1.91, and 1.70 Å, whereas the experimental r(H−H) are between 1.67 and 1.69 Å. Two other complexes with similar H−H distances, 1.73 and 1.76 Å, are **20** and **21**, where the coupling constants of +3.3 and −0.9 Hz would result in predicted r(H−H) = 1.75 and 2.29 Å, respectively, if used with eq 2′.

The recent work of Hush et al. on a range of dihydrogen complexes has shown that J_{HD} couplings can be reasonably accurately calculated using DFT.[23] We have carried out such calculations for complexes **5**, **9**−**11**, **13**−**22**, **25**, and **26**. The theoretical J_{HD} values are listed in Table 2 and are plotted in Figure 15. When r(H−H) > 1.3 Å, there is a good linear relationship between the experimental and calculated couplings in the form J_{HD}(exp) = 1.25J_{HD}(calc) + 0.63 (eq 4). For shorter H−H distances, the calculated couplings are close to the experimental values.

Acknowledgment. The author thanks NSERC and Research Corporation for funding.

Supporting Information Available: Atomic coordinates of all complexes optimized in this work and the basis sets used in the calculations. This material is available free of charge via the Internet at http://pubs.acs.org.

JA0465956

(31) (a) Barea, G.; Esteruelas, M. A.; Lledós, A.; López, A. M.; Oñate, E.; Tolosa, J. I. *Organometllics* **1998**, *17*, 4065. (b) The distance r(H−H) = 1.41 Å has been obtained taking into account the relaxation of the hydrides by other protons in **15** (R^* = 4.5 s^{-1}, calculated with the H−H distances from the optimized theoretical structure). The H−H distance of 1.36 Å in the original publication[31a] was obtained assigning all relaxation to the hydride−hydride interaction.
(32) (a) The distance r(H−H) = 1.53 Å has been obtained taking into account the relaxation of the hydrides by other protons in **16** (R^* = 0.84 s^{-1}, calculated with the H−H distances from the optimized theoretical structure). The H−H distance of 1.49 Å in the original publications[13a,d] was obtained assigning all relaxation to the hydride−hydride interaction. (b) The H−D coupling diminishes as temperature is lowered.
(33) Sabo-Etienne, S.; Rodriguez, V.; Donnadieu, B.; Chaudret, B.; el Makarim, H A.; Barthelat, J.-C.; Ulrich, S.; Limbach, H.-H.; Moise, C. *New J. Chem.* **2001**, *25*, 55.
(34) Gusev, D. G.; Lough A. J. *Organometallics* **2002**, *21*, 2601.
(35) Heinekey, D. M. *J. Am.Chem. Soc.* **1991**, *113*, 6074.
(36) Wilson, R. D.; Koetzle, T. F.; Hart, D. W.; Kvick, Å; Tipton, D. L.; Bau, R. *J. Am. Chem. Soc.* **1977**, *99*, 1775.
(37) Yandulov, D. V.; Huang, D.; Huffman, J. C.; Caulton, K. G. *Inorg. Chem.* **2000**, *39*, 1919.
(38) Hund, H.-U.; Ruppli, U.; Berke, H. *Helv. Chim. Acta* **1993**, *76*, 963.
(39) Gusev, D. G.; Nietlispach, D.; Vymenits, A. B.; Bakhmutov, V. I.; Berke, H. *Inorg. Chem.* **1993**, *32*, 3270.
(40) Lantero, D. R.; Motry, D. H.; Ward, D. L.; Smith, M. R., III. *J. Am. Chem. Soc.* **1994**, *116*, 10811.
(41) Ditzel, E. J.; Robertson, G. B. *Aust. J. Chem.* **1995**, *48*, 1183.
(42) Delpech, F.; Sabo-Etienne, S.; Donnadieu, B.; Chaudret B. *Organometallics* **1998**, *17*, 4926.
(43) Bautista, M. T.; Earl, K. A.; Maltby, P. A.; Morris, R. H. *J. Am. Chem. Soc.* **1988**, *110*, 4056.